

DEVELOPMENT OF A FAST-FEEDBACK DEFLECTOR MAGNET POWER SUPPLY FOR THE NEXT GENERATION HEAVY ION THERAPY*

K. Okamura[†], K. Takayama, High Energy Accelerator Research Organization, Tsukuba, Japan
 H. Kamezaki, Pulsed Power Japan Laboratory Ltd., Kusatsu, Shiga, Japan

Abstract

Application of a 10 Hz fast-cycling induction synchrotron (IS) to the next generation of heavy ion therapy called Energy Sweep Compact Rapid Cycling Hadron Therapy (ESCORT), where the ion beam with energy sweeping is delivered tracking a tumor target in a deformed and moving organ and monitoring the irradiation dose profile in a real-time during irradiation, is under investigation in the collaboration of KEK, SAMEER in India, and Subatech in France. To enable precise targeting, the final deflector magnet must adjust the beam on its irradiation position accurately by varying the polarity and peak current value for each pulse with the excitation pattern of the main magnet system. The developed power supply for the final deflector magnet makes this possible. This paper describes the initial experimental results obtained by combining a prototype power supply with a steering magnet.

INTRODUCTION

In the next-generation of particle therapy, the beam must be delivered tracking a cancer target in a deformed and moving organ and monitoring the irradiation dose profile in a real-time during irradiation. We have proposed and investigated Energy Sweep Compact Rapid Cycling Hadron Therapy (ESCORT) based on the acceleration principle of induction synchrotron (IS) [1, 2] with these features. Its driver is the rapid-cycling IS that is operated at 10 Hz. In the ESCORT system, the beam extracted from the

accelerator ring is scanned not only across the entire 2D cross-section of the irradiation target, but is also swept in depth; for this purpose, the two sets of deflector electromagnet shown in Fig. 1 are used in combination. The first set is a deflector that kicks the beam following the pre-programmed settings corresponding to the target irradiation position; it is called the program-operated deflector. The second set requires the maximum excitation value to be varied for each shot in response to signals from a real-time feedback computer while tracking the movement of the cancer target; we refer to this as the fast feedback deflector system (FFDS). This paper describes the magnet power supply in the FFDS that can provide the peak current amplitude and polarity in response to the command values varying each acceleration cycle.

EXPERIMENT WITH A PROTOTYPE POWER SUPPLY

Circuit Diagram

The proto type power supply was developed modifying the pattern waveform high-voltage dc power supply [3], which has the H bridge dc-dc converter scheme (Fig. 2). The key difference is that while the previous power supply used voltage control based on output voltage feedback, this power supply uses current control based on output current feedback.

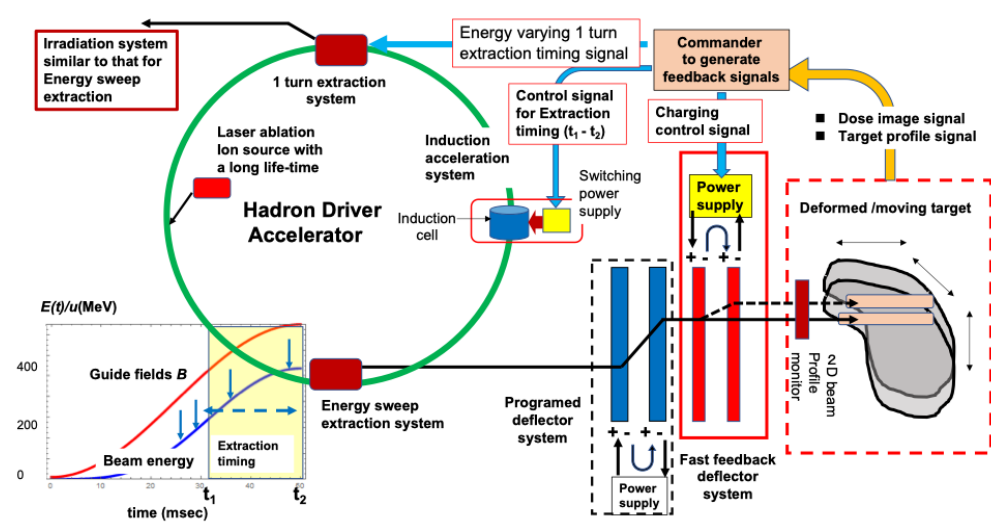


Figure 1: Conceptual diagram of the ESCORT.

* This study is supported by by Grant-In-Aid for Scientific Research (B) (KAKENHI No. 23H03666

[†]katsuya.okamura@j-parc.jp

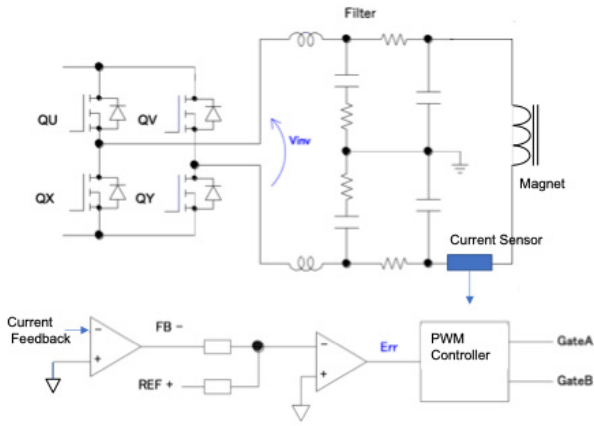


Figure 2: Schematic diagram of the prototype power supply.

Experiment

Experimental Setup Figure 3 shows the experimental setup. The digital pulse generator generates a pattern start signal for the arbitrary waveform generator and a gate enable signal for the prototype power supply.

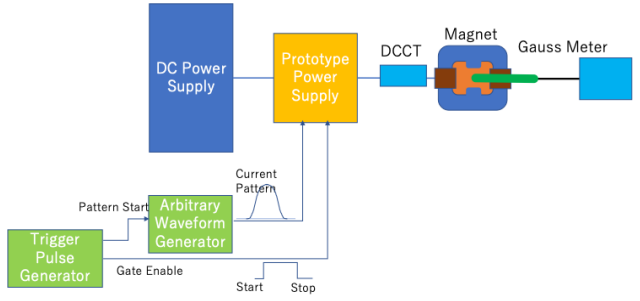


Figure 3: Experimental setup.

Current Tracking Accuracy and Ripples Figure 4 shows one of the current setup pattern, which is 10 Hz sinusoidal pattern with dc offset. The peak value was varied from -3 A to +3 A. Figure 5 shows the typical current deviation waveform, which is defined as the difference between setup current and output current with 100 Hz low pass filter. Both upper deviation and lower deviation were measured. An offset deviation was observed near the zero point at the start and end of the setup pattern. The measurement was executed 5 times at each setup current. Figure 6 shows the dependance of the current tracking accuracy on the setup current. The fact that there is a deviation even when the command value is 0 A is due to the above-mentioned offset.

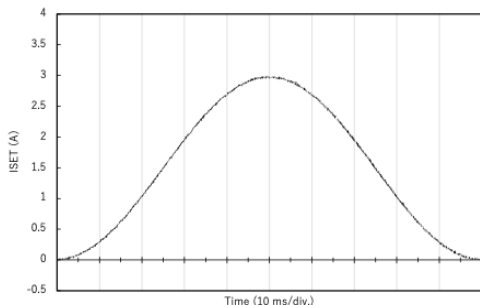


Figure 4: Single pulse current setup pattern.

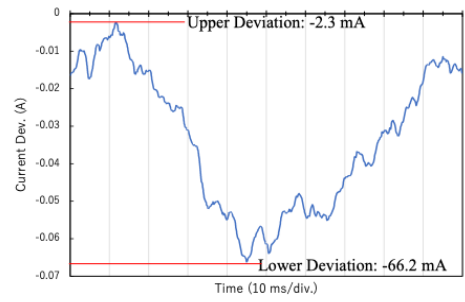


Figure 5: Typical current deviation waveform with the peak value of the setup current of 3A.

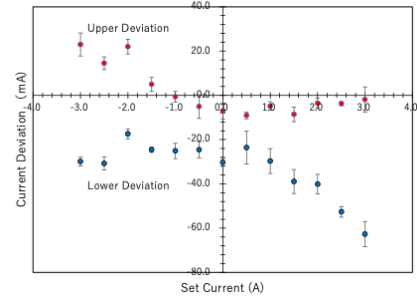


Figure 6: Current deviation as a function of the setup current.

Figure 7 shows the current ripple as a function of setup current with 1 kHz high pass filter. The current ripple does not depend much on setup current.

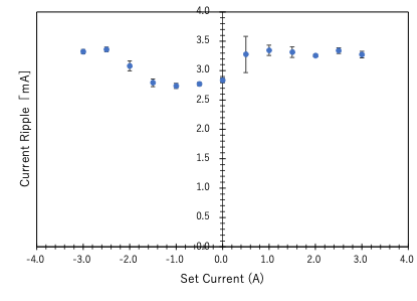


Figure 7: Current Ripple as a function of the setup current.

Magnetic Field Measurement An existing steering magnet made from thin laminated steel plates was used as a deflector magnet to minimize eddy current effects. Specifications of the magnet is shown in Table 1.

Table 1: Specifications of the Steering Magnet

Item	Value
Gap Length	160 (mm)
Pole Length	210 (mm)
Inductance	4.3 (H)
Resistance	11 (Ω)

The magnetic field was measured using a Gauss meter (F.W.BELL-610). The Hall probe was positioned at the center of the magnet gap. Magnetic field measurements were performed using two current patterns: a single-pulse pattern, identical to that used in the current tracking measurements, and a double-pulse pattern, which mimics to a requirement from the realistic varying feedback. Double-

pulse pattern measurements were performed to investigate the effect of magnetization induced by the preceding pulse on the subsequent pulse. In the double-pulse pattern, the peak of the first pulse was fixed at 3 A, while the peak of the second pulse was varied from 3 A to -3 A. Two examples of the double pulse patterns are shown in Fig. 8. In all measurements, a demagnetizing current, which consists of a series of alternating positive and negative pulses that gradually decay, was applied (Fig. 9) prior to the magnetic field measurement to eliminate the influence of the residual magnetic field.

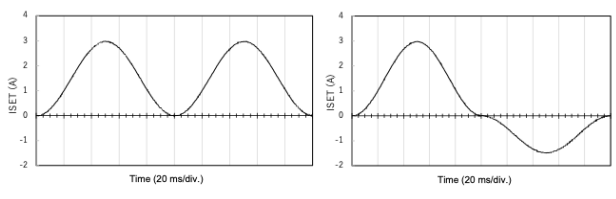


Figure 8: Two current pattern examples of double pulse magnetic field measurement. left: 3A / 3A. right: 3 A / -1.5 A.

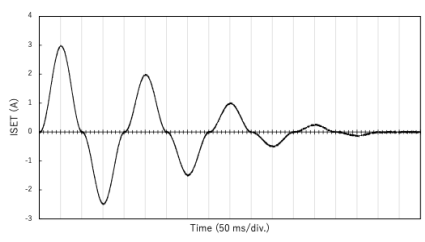


Figure 9: Demagnetizing current pattern.

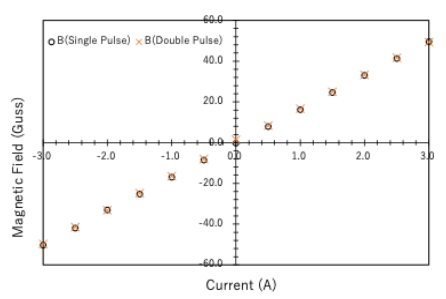


Figure 10: Magnetic field vs. current.

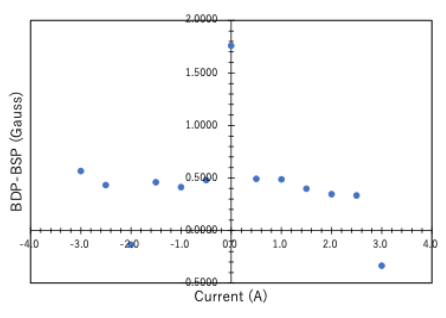


Figure 11: Magnetic field difference between single pulse and double pulse.

Figure 10 compares the magnetic field measurement results obtained using a single pulse with those obtained using a double pulse. There is little difference between the

two sets of results. Figure 11 shows the difference between the single-pulse and double-pulse measurements. In general, the double-pulse measurements are about 0.5 gauss higher, but it can be seen that only when the current is 0 A the double-pulse measurement is 1.7 gauss higher. This distinct phenomenon suggests the influence of the residual magnetic field.

DISCUSSION

Feedback Position Error Caused by Power Supply Deviation

Here, we examine the effect of power supply tracking error on beam deflection error. Figure 12 shows the geometric assumptions.

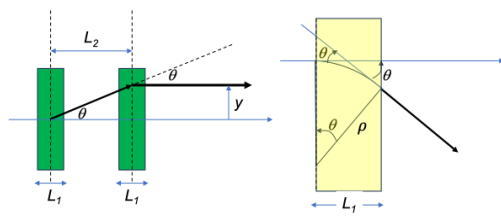


Figure 12: Geometric assumptions for discussing deflection errors.

As can be seen from Figure 12, the relationship between the magnet length L_1 , bending radius ρ and the deflection angle θ is expressed as follows.

$$L_1 = \rho \cdot \sin \theta \approx \rho \cdot \theta . \quad (1)$$

When the spacing between the deflection magnet pair is denoted by L_2 , the deflection y is

$$y = L_2 \tan \theta \approx L_2 \cdot \theta \approx L_1 \cdot L_2 / \rho . \quad (2)$$

If we denote the error in the magnetic field by ε , bending radius ρ can be expressed shown in Eq. (3).

$$\rho = \frac{1}{c} \cdot \left(\frac{A}{Q} \right) \cdot \left(\frac{mc^2}{e} \right) \cdot \left(\frac{\beta\gamma}{B_0(1+\varepsilon)} \right) \approx \rho_0(1 - \varepsilon) . \quad (3)$$

Here, Q is the charge, A is the mass number, γ is the Lorentz factor. And B_0 and ρ_0 are magnetic field and bending radius in the absence of errors, respectively. Therefore the deflection length with the field error is

$$y = L_1 \cdot \frac{L_2}{\rho_0} \cdot (1 + \varepsilon) = y_0(1 + \varepsilon) . \quad (4)$$

It is concluded that the error in deflection is comparable to that in the magnetic field. According to the results of this experiment, the error in the magnetic field depends almost entirely on the current tracking performance and, including the offset, is approximately 1–2%, which is sufficiently acceptable.

CONCLUSION

A prototype of the fast-feedback deflector magnet power supply was demonstrated and tested in combination with the steering electromagnet. The results confirmed that it was sufficiently responsive to current commands that varied with each acceleration cycle.

REFERENCES

- [1] L. K. Wah, T. Monma, T. Adachi, T. Kawakubo, T. Dixit, and K. Takayama, “Compact hadron driver for cancer therapies using continuous energy sweep scanning,” *Phys. Rev. Accel. Beams*, vol. 19, no. 4, Apr. 2016.
[doi:10.1103/physrevaccelbeams.19.042802](https://doi.org/10.1103/physrevaccelbeams.19.042802)
- [2] K. Takayama, T. Kawakubo, T. Adachi, T. Dixit, and A. Shaikh, “Energy-varying beam extraction assisted by large momentum deviation and charge exchange,” *Phys. Rev. Accel. Beams*, vol. 24, no. 1, Jan. 2021.
[doi:10.1103/physrevaccelbeams.24.011601](https://doi.org/10.1103/physrevaccelbeams.24.011601)
- [3] K. Okamura, K. Takayama, A. Tokuchi, and T. Yoshimoto, “A study on the pattern waveform high-voltage power supply for the rapid cycling induction synchrotron”, in *Proc. IPAC'25*, Taipei, Taiwan, Jun. 2025, pp. 1830-1832.
[doi:10.18429/JACoW-IPAC2025-WEPB043](https://doi.org/10.18429/JACoW-IPAC2025-WEPB043)